We are IntechOpen, the world's leading publisher of Open Access books Built by scientists, for scientists

6,900
Open access books available

185,000
International authors and editors

200M
Downloads

Our authors are among the

154
Countries delivered to

TOP 1%
most cited scientists

12.2%
Contributors from top 500 universities



WEB OF SCIENCE™

Selection of our books indexed in the Book Citation Index in Web of Science™ Core Collection (BKCI)

Interested in publishing with us?
Contact book.department@intechopen.com

Numbers displayed above are based on latest data collected.
For more information visit www.intechopen.com



3

Fabrication of InGaN-Based Vertical Light Emitting Diodes Using Electroplating

Jae-Hoon Lee[1] and Jung-Hee Lee[2]
[1]*GaN Power Research Group, R&D Institute, Samsung LED Company Ltd., Suwon,*
[2]*Electronic Engineering & Computer Science, Kyungpook National University, Daegu, Korea*

1. Introduction

Group III–nitride semiconductors and their ternary solid solutions are very promising as the candidates for both short wavelength optoelectronics and power electronic devices (Nakamura et al. 1997; Nakamura et al. 1995; Lee, et al. 2010; Youn, et al. 2004). The AlGaN/GaN heterostructure field effect transistors (HFETs) have a great potential for future high-frequency and high-power applications because of the intrinsic advantages of materials such as wide bandgap, high breakdown voltage, and high electron peak velocity (Smorchkova et al. 2000). Major developments in wide-gap III-nitride semiconductors have led to commercial production of high-brightness light emitting diodes (LEDs). The InGaN-based LEDs have already been extensively used in full-color displays, traffic displays, and other various applications such as projectors, automobile headlights, and general lightings. In particular, white LEDs based on InGaN/GaN quantum well heterostructure are regarded as the most promising solid-state lighting devices to replace conventional incandescent or fluorescent light. It is required, however, to reduce the high dislocation density due to large lattice mismatch between GaN epitaxial layer and sapphire substrate and to increase the light extraction efficiency for fabricating high-performance LEDs. Epitaxial lateral overgrowth (ELOG) or pendeo epitaxy (PE) has been used to partially overcome the problems (Sakai et al. 1997; Zheleva et al. 1997). Although the ELOG and PE process can dramatically decrease dislocation density, the related growth process is complicated and time consuming. Recently, it has been reported that one can not only reduce the threading dislocation density in GaN films, but also enhance the light extraction efficiency by using patterned sapphire substrate (PSS) (Yamada, et al. 2002; Tadatomo, et al. 2001; Wuu, et al. 2006). The PSS technique has attracted much attention for its high production yield due to the single growth process without any interruption. Future demands for these and more advanced applications will require higher light output with lower power consumption. The refractive index of nitride films (n = 2.4) is higher than that of air (n = 1) and sapphire substrate (n = 1.78). The critical angle of the escape cone is about 23°, which indicates that about only 4% of the total light can be extracted from the surface (Huh, et al. 2003). Most of the generated lights in the active layer is absorbed by the electrode at each reflection and gradually disappear due to total internal reflection. In order to improve the light extraction efficiency, it is very important to find the escape cone which the photons generated from LEDs experience multiple opportunities. Several previous works have reported that one can increase the light extraction efficiency of

nitride-based LEDs by roughening the sample surface. However, the surface texturing is difficult in conventional LED because the p-GaN top layer being too thin for texturing and the sensitivity of p-GaN to plasma damage and electrical deterioration. It is also well known that poor heat dissipation has been the main problem in the development of high-power InGaN/sapphire LEDs. For a conventional nitride-based LED, the generated heat is dissipated through the path from sapphire to silver paste and then to heat sink. The poor thermal conductivities of sapphire (~35 W/mK) and silver paste (2-25W/mK) limit heat flow and dissipation, resulting in increased junction temperature of the device due to Joule heating at the p-n junction. Recently, high efficiency GaN based LEDs was fabricated using the laser lift-off (LLO) technique (Fujii, et al. 2004; Wang, et al. 2005; Wang, et al. 2006). The LLO process can enhance the light output power, the operating current and the heat sink of fabricated vertical type LED (VT-LED). The other advantage of VT-LED is room for roughening top surface compared to conventional lateral LED. It has been reported to produce a roughened VT-LED surface with conlike feature and microns arrays using photoelectrochamical etching and plasma etch process, respectively. However, since these approaches involve difficult and complicated fabrication process, improvement is still required for higher device performance. In this work, we have proposed a new method utilizing surface texture of vertical type LEDs by using cone-shape patterned sapphire substrate (CSPSS) for the purpose of increasing extraction efficiency (Lee, et al. 2006; Lee, et al. 2008; Lee, et al. 2009) Compared to conventional roughening process, the proposed method is simple and highly reproducible due to forming patterns neatly designed on sapphire before GaN growth. In this chapter, firstly the history and important properties of the group III-nitrides is briefly reviewed, then the fabrication of the InGaN-based VT-LED was presented, finally a conclusion is drawn.

2. Evolution of III-nitride materials

GaN was first created in 1932 by Johnson at the University of Chicago by reacting ammonia gas with solid gallium at temperature of 900-1000℃ (Johnson et al. 1932). The GaN synthesis technique was also used to study the crystal structure and lattice constant by Juza in 1938 and to study the photoluminescence spectra by Grimmeiss in 1959 (Juza, et al. 1938; Grimmeiss, et al. 1959). Maruska and Tietjen deposited the first large area GaN layers on sapphire in 1969 using vapor-phase transport in chlorine (Maruskam, et al. 1969). This earliest research on GaN was directed at understanding the properties of the material and learning how to design the material for specific uses. All the early GaN was very conductive as grown, and it was realized that these crystals were n-type with high carrier concentration owing to the highly defective nature of the crystal (Pankove, 1997). Because the work on GaN had early been focused on its potential for optical sources, p-type GaN was required in order to make p-n junction emitters, so much effort was focused in this area. Pankove et al. were successful in fabricating the first blue GaN LED (Pankove, et al. 1972). It was as metal/insulating GaN:Zn/n-GaN (MIS) diode. The n-GaN layers contained different concentration of Zn. The wavelength of the emitted light depended on the Zn concentration. Until the late 1970s the quality of GaN was not very good. The results of optical and electrical measurements were not reproducible. Yoshida et al. deposited an AlN buffer layer to overcome the nucleation problems of GaN grown directly on a sapphire substrate in 1983 (Yoshida, et al. 1983). This buffer layer technique was very effective in improving the overall material quality on sapphire. The two-step method was investigated and perfected by Akasaki, Amano and co-worker in 1988/1989 (Amano, et al. 1986). In the first step a thin

buffer layer of AlN is grown on the sapphire substrate at a low temperature of ~ 500℃. The GaN layer is grown on the buffer layer. This importance accomplishment allowed GaN to be grown with much higher crystal quality than was previously available. The world wide attention on the research of group III-Nitrides were stimulated by the success in the material quality improvement with low temperature GaN nucleation layer by Nakamura in the early 1990's and later by the success in blue LEDs and LDs by Nakamura, leading toward the fundamental understanding of group III-Nitride material system (Nakamura, 1991; Nakamura, et al. 1996). The GaN-based FETs were also fabricated about the same time, i.e., in 1993 (Khan, et al. 1993). Fabrication of a heterostructure bipolar transistor using p-type 6H SiC as the based and n-type GaN as the emitter was reported in 1994 (Pankove, et al. 1994). Metalorganic chemical vapor deposition (MOCVD) has been the most popular growth technique for nitride growth and has been the choice for several electronic and optoelectronic devices such as HEMTs, HBTs, LEDs, and LDs.

2.1 Important properties of III-nitride materials

The III-nitride group of materials includes GaN, AlN, InN, and their alloys. The bandgap of the nitride group of materials is direct and have different band gaps ranging from 6.2 eV for AlN down to 0.7 eV for InN. This gives a tremendous optical range for III-nitride materials, from yellow to ultraviolet. The large bandgap and strong termodynamical stability of the III-nitride material system point to promising high power and high-temperature electronic device applications. Nitride materials are also extremely resilient to harsh chemical environments, giving the possibility for use in environments where the more traditional III-V materials are unable to perform. The most thermodynmically stable form of the nitride materials is the wurtzite or hexagonal form. This result in the familiar hexagonal close pack (HCP) model of alternating planes of Ga and N atoms stacked in an ABABAB sequence. The crystal planes in the wurtzite system are given using the Miller-Bravis index system of [ijkl] with k = - (i + j). Further detail on HCP and hexagonal crystal notation can be found in the classic textbook "Introduction to Solid State Physics" by Charles Kittel (Kittel, 1995). Nitrides can also be forced to grow in a zincblend form by using cubic substrates such as (001) Si and GaAs. The stacking sequence in this case is ABCABC. However, although the electrical properties of cubic III-nitrides are in theory expected to be better than for hexagonal GaN, in practice cubic III-nitrides are generally not as high quality as the wurtzite form and often contain a mixture of both cubic and wurtzite phases (mixed phase). The structural properties of the cubic nitrides can be found in Ref (Gil, 1998).

The most common substrate for GaN epitaxial growth is sapphire. It was the substrate used during the first attempts at GaN epitaxy during the late 1960's and has remained as the leading choice to this day. The attraction to sapphire for GaN epitaxy stems from its high melting point, chemical stability, availability of large wafer sizes, very high quality crystals, and low wafer cost. However, sapphire has a large lattice and thermal mismatch with GaN, leading to high defect density (~10^9/cm^2) in the GaN film and limiting the maximum layer thickness to less than 10 μm. In addition, the low thermal conductivity of sapphire limits heat dissipation through the substrate, imposing severe limits for power devices on this substrate. Despite these difficulties, sapphire remains as leading candidate for basic of III-nitride epitaxy due to wide availability and low cost. In the case of growth on c-plane sapphire, a 30° rotation around the c axis occurs for GaN Epitaxy, resulting in an effective

lattice constant that is $1/\sqrt{3}$ less than a sapphire. The resulting lattice mismatch is ~ 13%. In addition, on c-plane sapphire, the thermal expansion mismatch is -25.5 %.

Table 1 lists some of the common electronic properties of the III-nitride group of materials (for comparison, properties of Si, GaAs, and SiC are also included) (Levinshtein, et al. 2001). As can be seen, both SiC and the nitride group have larger bandgap energy than either Si or GaAs. The larger bandgap and high breakdown field of these materials allow SiC and Nitride based electronic devices to operate at higher temperatures and higher powers than Si or GaAs based devices. In addition, while SiC has a badgap near that of GaN, the III-nitrides group has three distinct advantages over SiC devices. First, the nitride groups of materials have direct transition bandgap, allowing for use in optical devices such as lasers and LEDs. Secondly, the nitride group has the availability of ternary (AlGaN, InGaN) and quaternary (AlInGaN) compounds leading to a more versatile bandgap range (0.7~6.2) than SiC alone and allowing for bandgap engineering in both optical and electronic application. Finally, the nitride ternary and quaternary compounds can be used for heterojunction

Material	**Bandgap (eV)**	**Lattice constant (Å)**	**Lattice mismatch with GaN(%)**	**Thermal Conductivity at 300K (W/cmK)**	**Thermal expansion coeff. (10^{-6}/K)**
AlN	6.2	a=3.112 c=4.982	2.48	2.0	4.2 5.3
GaN	3.44	a=3.1891 c=5.1855	0	1.3	5.59 3.17
InN	0.7	a=3.548 c=5.7034	-10.12	0.8	5.7 3.7
6H SiC	3.03	a=3.081 c=15.117	3.51	4.9	4.2 4.68
Al_2O_3	9.0	a=5.431 c=12.982	13.9	0.3	7.5 8.5
Si	1.12	a=5.431	-16.96	1.3	3.9
GaAs	1.42	a=5.653	-20.22	0.5	6.7

Material	**Electron mobility (cm^2/Vs)**	**Hole mobility (cm^2/Vs)**	**Saturated drift velocity (10^7cm/s)**	**Breakdown field (MV/cm)**	**Melting Point(℃)**
AlN	135	14	1.4	4-12	3124
GaN	300-1000	<200	2.5 (calc) 2.0 (exp)	5.0	2518
InN	1000-1900	-	2.5	5.0	1873
6H SiC	400	50	2.0	3-5	>2000
Al_2O_3	-	-	-	-	2015
Si	1500	450	1.0	0.3	1412
GaAs	8500	400	1.0	0.4	1240

Table 1. Crystal and electrical properties of III-nitrides, SiC, Si and GaAs (Kittel, 1995; Gil, 1998; Levinshtein, et al. 2001).

(HFET, HBT) and quantum well based devices. SiC does not have any alloys systems, relegating use of SiC to native oxide based devices (MOSFETs). As seen in Table 1, the undoped electron and hole mobility of the III-nitrides and SiC are relatively low compared to Si and GaAs. The electron mobility for unintentionally doped (UID) single GaN layers on either sapphire or SiC average about 300~400 cm^2/Vs. Undoped mobility in these materials are normally limited by defect related scattering of defect hoping (Ng, et al. 1998). The highest reported mobility for MOCVD grown GaN was ~ 900 cm^2/Vs (Nakamura, et al. 1997). The maximum calculated phonon-limited mobility in GaN is ~1350 cm^2/Vs for electrons and ~200 cm^2/Vs for holes (Look, et al. 2001). Light n type doping of GaN (~$1 \times 10^{17}/cm^3$) results in improved mobility due to screening of dislocations and decreased defect-related conductivity. Further doping of the material leads to mobility degradation due to ionized impurity scattering. It should be noted that much higher mobility is possible (1500~2000 cm^2/Vs) in GaN heterostructures by forming a high mobility two dimensional electron gas (2DEG) channel. Another important property for high frequency operation is the saturation electron drift velocity. This parameter gives the average electron velocity at high electric fields. The high saturated drift velocity of III-nitrides leads to applications at high frequencies than can be achieved from Si. As seen in Table 1, the calculated value of GaN electron velocity is 2.5×10^7 cm/s, although experimental evidence is closer to 2.0×10^7 cm/s (Wraback, et al. 2000) in bulk GaN and near 1.0×10^7 cm/s for sub-micron HFET devices (Ridley, et al. 2004). The discrepancy between theory and experimental velocity saturation was accounted for in bulk GaN as due to high defect density not accounted for in theory and in case of HFET devices as due to hot carrier effects. In addition, the wide bandgap and high breakdown field give the possibility or nitride application at both high-frequency and much higher power levels than Si or traditional III-V materials.

3. Fabrication of InGaN-based vertical type light emitting diodes

The epitaxial layers were grown both on CSPSS and conventional sapphire substrate (CSS) by using a metal organic chemical vapour deposition (MOCVD). Figure 1 shows a schematic layer structure and procedure of fabricated VT-LEDs employing selective Ni electroplating and LLO techniques. The LED structure consists of an undoped GaN layer, a Si-doped n-GaN layer, five layers of InGaN/GaN multiple quantum well (MQW), and an Mg-doped p-GaN layer. The grown sample was patterned with 230×640 μm^2 size by a standard photolithographic process. The full mesas were defined by ICP-RIE from p-GaN to sapphire bottom to prevent GaN film from breaking due to different stress between sapphire and GaN film for LLO process. A metal scheme of Ni/Ag/Pt was deposited onto the p-GaN top surface to serve as p-ohmic contact and reflector metal. A TiW and Ti/Au layers were subsequently deposited as a barrier layer and an adhesive layer for the nickel electroplating. To sustain the remaining thin LED structure after the removal of sapphire substrate, the thickness of a nickel layer is around 80 μm. To remove the sapphire substrate, a 248 nm KrF excimer laser with pulse width of 25 ns was used for LLO process. Finally, n-contact pad region was defined by ICP-RIE to expose the n-GaN layer and Cr/Au layer was then deposited on n-GaN without additional semitransparent contact layer. For the characterization of the surface morphology of the grown layers, we used a scanning electron microscope (SEM). The crystal quality of the grown films was investigated by both X-ray diffraction (XRD) and transmission electron-microscopy (TEM). The output power of the fabricated VT-LEDs was measured under DC bias at room temperature.

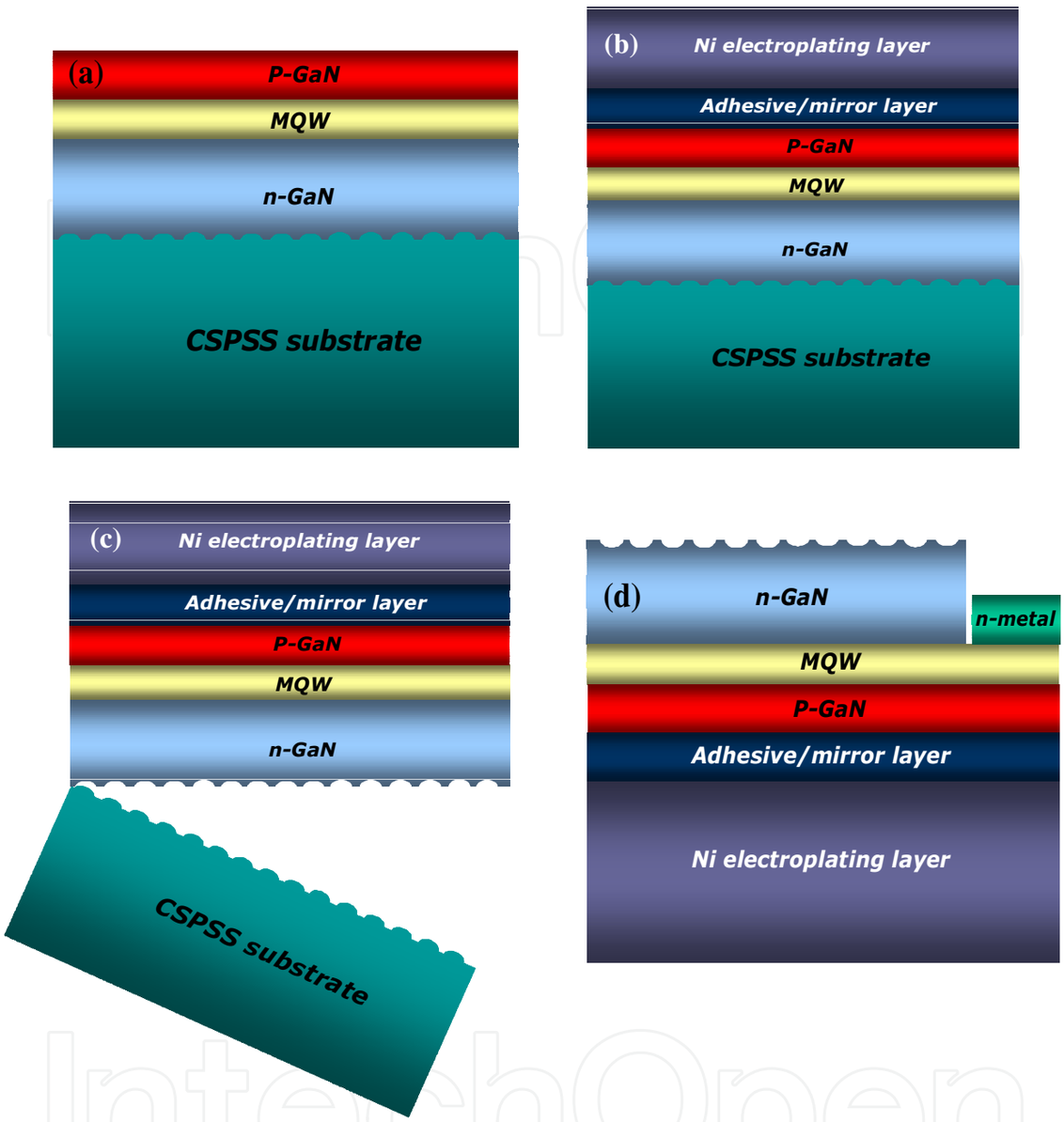


Fig. 1. Schematic layer structure (a) and procedure of fabricated VT-LEDs employing selective Ni electroplating and LLO techniques. (b) p-GaN ohmic contact/mirror layer and Ni electroplating processing, (c) Samples at the LLO processing stage. (b) Samples at the n-GaN ohmic contact processing.

3.1 GaN film on patterned sapphire substrate

Figure 2 shows a scanning electron microscope (SEM) image of the fabricated CSPSS process. The preparation of the CSPSS is as follows [Lee, et al. 2008]. After a photoresist (PR) with 3.5-μm thickness had been coated on a c-plane (0001) sapphire substrate, the PR was patterned first to be a rectangular shape [Fig. 2(a)] with different interval and reflowed during a hard-baking process at 140 ℃ to make a cone shape as shown in Fig. 2(b). The

sapphire substrate was then etched by using inductively coupled plasma reactive ion etching employing reactive Cl_2 gas. The diameter and interval of each cone-shaped pattern were 3 and 1 μm, respectively. The height of the cone shape was about 1.5 μm. The epitaxial layers were grown both on CSPSS and conventional sapphire substrate (CSS) by MOCVD. In the initial stage of the growth on CSPSS, the GaN layer starts to grow only on the etched flat basal sapphire surface, quite differently from the growth mode on the conventional PSS, because there is no preferential growth plane on the cone-shape-patterned region. Similarly to the ELOG, this selective growth on CSPSS prevents the dislocation generated during the initial stage of the growth from propagating further into the patterned area when the growth proceeds laterally toward the cone region, decreases the dislocation density, and hence improves the crystal quality of the grown film.

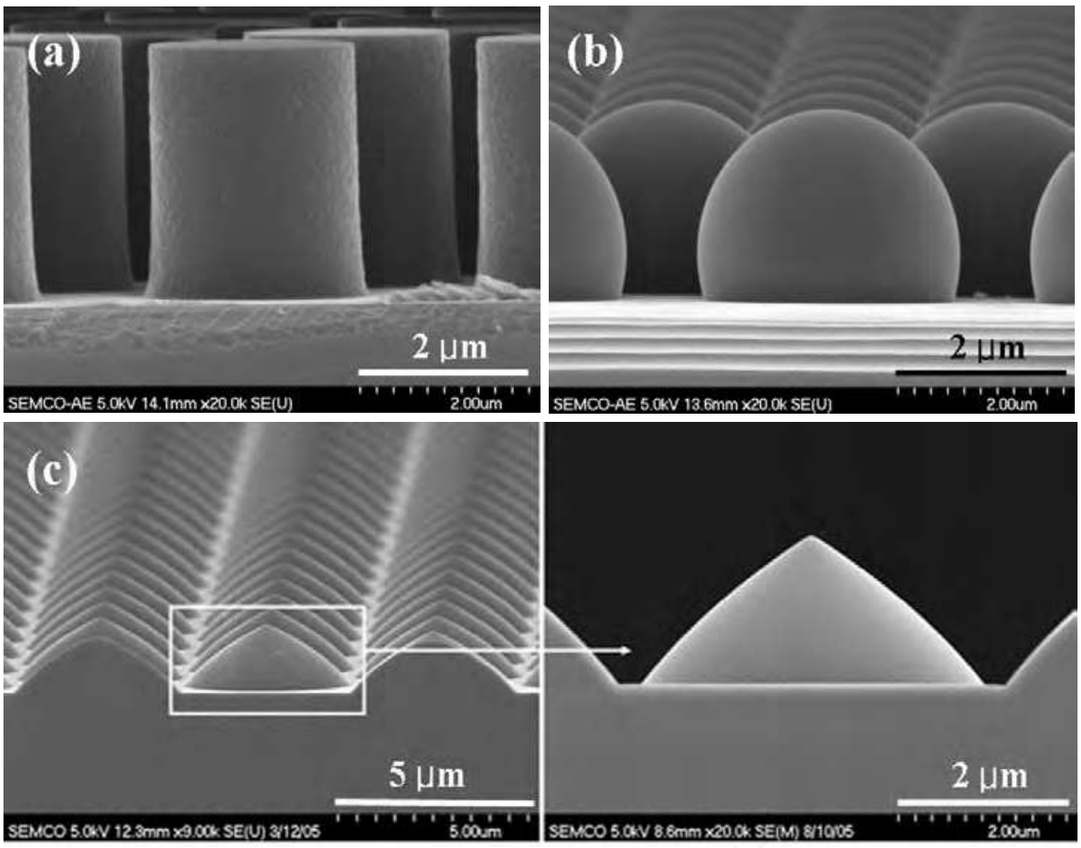


Fig. 2. SEM images of the fabricated CSPSS process. (a) PR patterning, (b) reflow process, (c) fabricated CSPSS.

The time evolution of interference micrographs for a GaN surface grown on a CSPSS is shown in Fig. 3, i.e., after the growth of the initial buffer layer at low temperature [Fig. 3(a)], after temperature ramping (annealing the buffer layer) [Fig. 3(b)], and after 10- and 30-min growth of the epitaxial layer [Fig. 3(c) and (d)]. In general, the III-nitride layer preferentially grows on the (0001) crystallographic c-plane of a sapphire substrate. Although there is no growth plane in the cone-shape-patterned region, the low-temperature GaN amorphous buffer layer is well formed on the plane and patterned sapphire region as shown in Fig. 3(a).

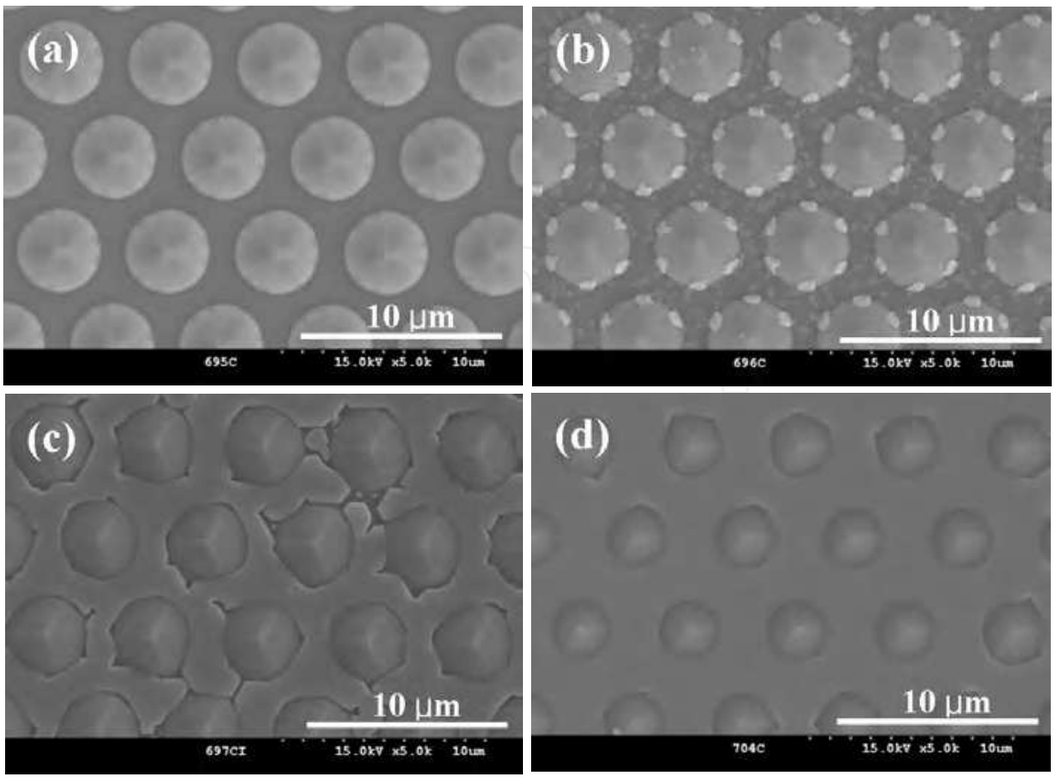


Fig. 3. Time evolution of interference micrographs for a GaN surface grown on a CSPSS. (a) buffer, (b) annealing, (c) 10 min., (d) 30 min.

When the temperature increases from low temperature (550 ℃) to high temperature (1020 ℃) in the ramping stage of the growth, the random recrystallized GaN islands are formed on the etched flat basal sapphire surface, which is similar to a typical growth mode on the CSS. In the cone-shape-patterned region, however, the larger regular GaN islands are formed on the six corners of a hexagon-shaped cone as shown in Fig. 3(b), which explains that Ga species tend to migrate from the top region of the cone surface to the bottom region of the cone as increasing temperature (Simeonov, et al. 2006; Sugiura, et al, 1997; Sumiya, et al. 2003). In the initial stage of the high-temperature growth on the CSPSS, therefore, the coalescence starts on the etched flat basal sapphire surface, indicating that the growth mode on the CSPSS is considerably different from that on the conventional PSS such as stripe, hexagonal, or rectangular geometry. As expected, the growth of GaN on the CSPSS was only initiated from the etched basal surface with the (0001) crystallographic plane because there was no growth plane in the cone-shape patterned region as shown in Fig. 3(c). As the growth proceeds, the growth also laterally propagates toward the peak of the cone as shown in Fig. 3(d). This lateral growth greatly decreases the dislocation density in the grown film, similarly to the ELOG mode. This also enables reducing the time required in obtaining a smooth growth surface over the patterned region, compared to that for those grown on a conventional PSS, where the growth starts both on the etched and nonetched regions at the same time as shown in Fig. 4. Figure 5 (a) shows the cross-sectional TEM images under g = 0002 two-beam condition of the interface region between the CSPSS and a GaN layer grown on it, demonstrating that the ELOG-like mode on the CSPSS effectively suppresses the

propagation of dislocation into the cone region, even though many dislocations were observed in the film grown on the basal plane of the sapphire. This reduction of dislocation was also confirmed by performing a cathodoluminescence (CL) measurement at room temperature as shown in Fig. 5(b, c). In bright regions, a radiative process dominates over a nonradiative process because of the lower density of structural defects. The dark spot density in the film grown on a CSS is roughly estimated to about 7×10^8 cm^{-2}. Apparently, the dark spot density in the film grown on a CSPSS was decreased to about 2×10^8 cm^{-2} in number.

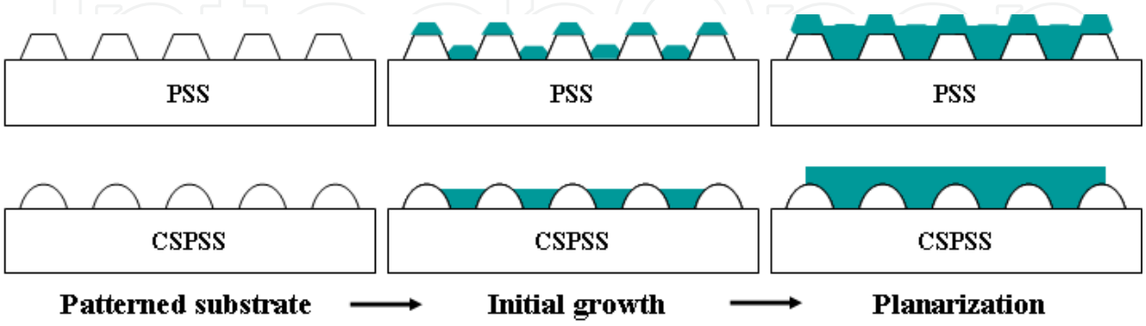


Fig. 4. Schematic view of the planarization of GaN grown on the conventional PSS and on the proposed CSPSS.

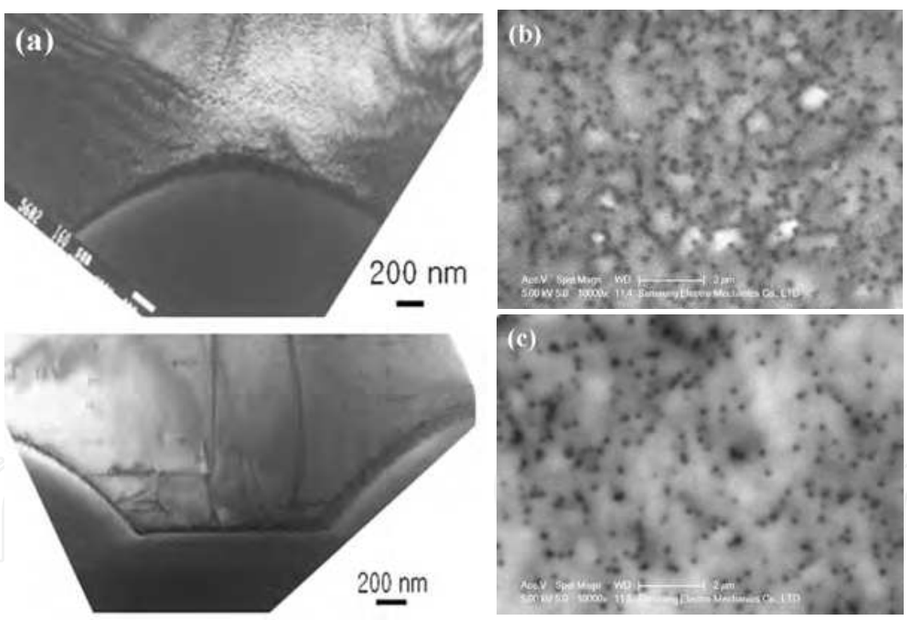


Fig. 5. TEM image (a) of a film grown on a CSPSS and CL image of (b) film grown on a CSS and (c) film grown on a CSPSS.

3.2 Characteristics of GaN films on CSPSS

Room temperature photoluminescence (PL) spectra for both InGaN/GaN samples grown on CSS and CSPSS are shown in Fig. 6. The band-edge emission intensity of the sample grown CSPSS was about four times higher in magnitude than that of the sample grown on CSS. The full width half maximum (FWHM) values of samples gown on CSS and CSPSS are 19 and 17

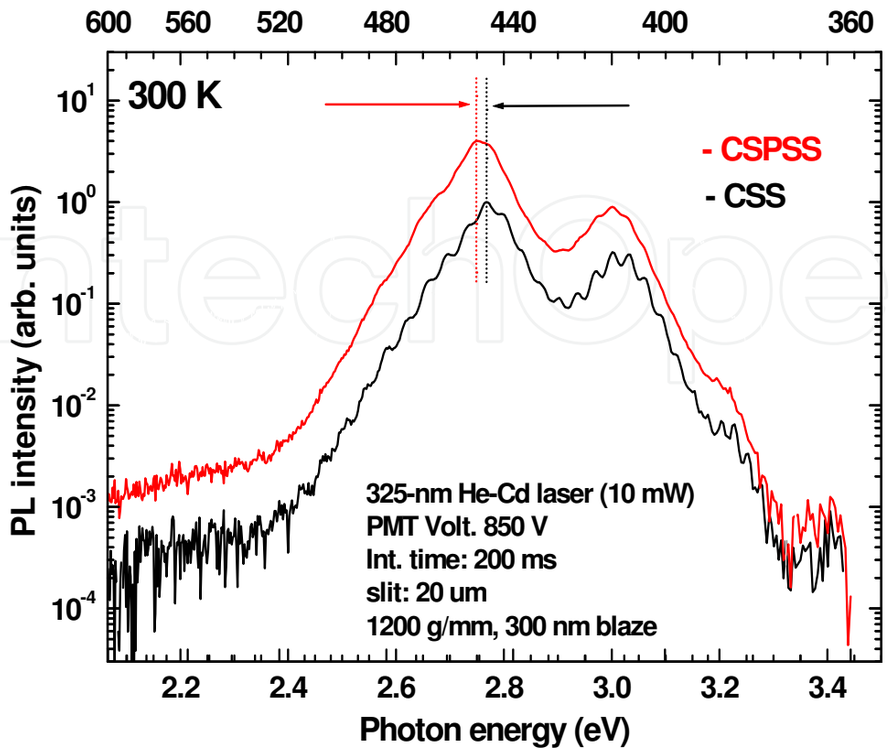


Fig. 6. PL measurements of InGaN/GaN films grown on a CSS and a CSPSS.

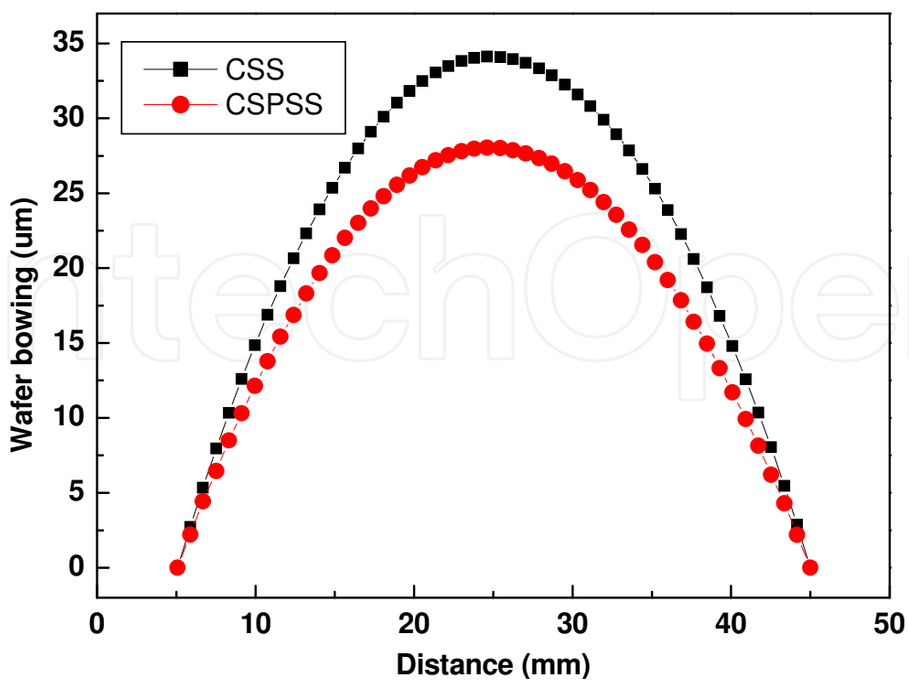


Fig. 7. Wafer bowing of films grown on CSS and CSPSS.

nm, respectively. In conjunction with a considerable enhancement in emission intensity and FWHM in PL, it is clear that the crystal quality of the film grown on CSPSS is improved. The typical corresponding spectral PL peak wavelength from the InGaN/GaN MQWs was shifted from 448 nm for film grown on CSS to 451 nm for film grown on CSPSS. In our previous work (Lee, et al. 2008), we reported that the surface geometry of CSPSS may be adequate for the easy relaxation of compressive strain during the growth on sapphire. The lattice constant c of films grown on CSPSS is very close to lattice constant of the bulk GaN of 5.185 Å, while the lattice constant of the GaN film grown on CSS exhibits a relatively large lattice constant. The slight red shift in PL for the film grown on CSPSS is due to the reduced band-gap energy which is caused by the decreased lattice constant c. The reduction of compressive stress in the films grown on CSPSS was also confirmed by thin film stress measurement using FLX-2320S as shown in Fig. 7. The bowing and stress of the 5.12 μm-thickness film grown on CSS were 34 μm and -437 Mpa with sapphire Young's modulus of 4.08 MPa. On the other hand, the values were reduced to 28 μm and -364 Mpa for the film with thickness of 5.48 μm grown on CSPSS. Consequently, the ELOG-like mode for the GaN layer grown on CSPSS results in less lattice mismatch and incoherency between the GaN layer and the sapphire substrate.

3.3 Role of electroplating

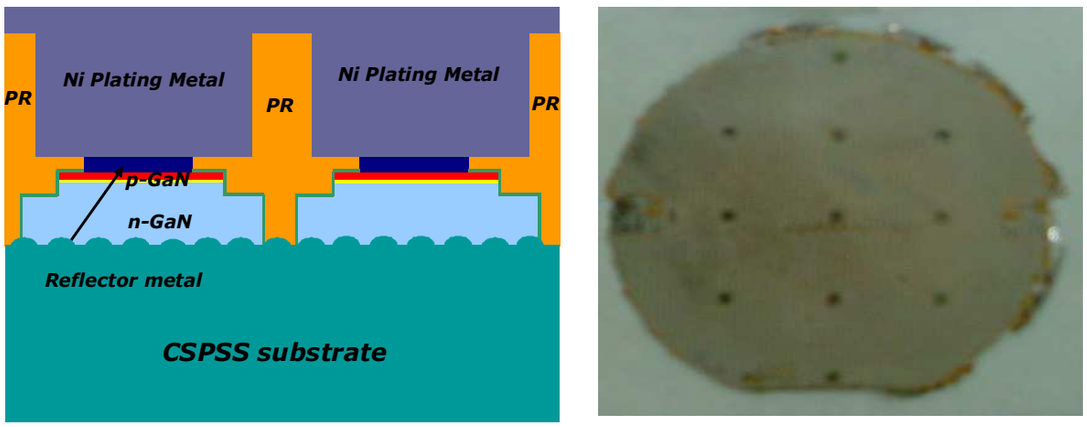
High power GaN-based LEDs are essential for next-generation lighting applications. Essentially, maintain the effective power conversion efficiency (λ=Po/Pe, i.e., the ration of the light output power Po to the electrical power Pe) at a high injection current density is the key to boost their development. However, it is inevitable that the excessive Joule heating from the inherent parasitic resistance and current crowding due to the insulating sapphire substrate in the operation region would eventually decrease radiative recombination efficiency and in turn decrease light output power conversion efficiency. To resolve this situation, the use of a metallic substrate with laser lift-off technology to realize VT-LEDs has been proposed and has attracted much attention (Fujii, et al. 2004; Wang, et al. 2005; Wang, et al. 2006).

3.4 Patterned Ni electroplating

The electroplating process was conducted under a current of around 1.65A with the plating solution kept at about 55 ℃, which contains nickel sulphate, nickel chloride, boric acid, water, and some additives to improve surface roughness. The growth rate of nickel layer is about 1000 nm/min. Our experimental results reveal that a nickel layer with a thickness of about 60-80 μm is mechanically strong enough to sustain stress after the removal of sapphire substrate. Figure 8 shows the bowing of film after normal Ni electroplating. The curvature of the bowing increases as thickness of Ni electroplating is increases. This is because the residual compressive stress in the GaN layer, caused by different thermal expansion coefficients between the GaN film and the Ni electroplating substrate. Therefore, the appropriate condition of electroplating is required to prevent the bowing of film. To obtain a flat surface, a patterned Ni electroplating was proposed. Figure 9 shows the schematic view of patterned Ni electroplating. The stress between the GaN and the Ni electrode films was released by using the patterned electroplating through thicker photo resistor (PR), which is resulted in flat film as shown in Fig. 9 (b).



Fig. 8. The bowing of films after normal Ni electroplating.



(a) (b)

Fig. 9. Proposed patterned Ni electroplating (a) schematics of patterned Ni electroplating, (b) The bowing of films after patterned Ni electroplating.

3.5 Concaved surface transfer after Laser lift-off

Figure 10 shows the formation of concaved surface transferred from CSPSS after LLO. To remove the sapphire substrate, A 248 nm KrF excimer laser with a single pulse of 25 ns. The incident laser fluence was set to a value of about 0.75J/cm^2 which was based on our earlier established threshold laser fluence by taking into account the attenuation of sapphire and the reflection in the sapphire/GaN interface. The laser beam with a size of 1 mm × 1mm was incident from the polished backside of the sapphire substrate into the sapphire/GaN interface to decompose GaN into Ga and N_2. Figure 10 (b), (c) show the SEM images of top surface of CSPSS substrate and removed GaN films after the LLO process. A finite amount of Ga residues appears on the top surface of the GaN and CSPSS substrate. The remaining Ga droplets on the transferred GaN surface were removed by a wet chemical etching using diluted HCl:H_2O (1:2) solution for 1 min. Figure 10 (d) shows the SEM photographs of top surface of removed GaN after the LLO process.

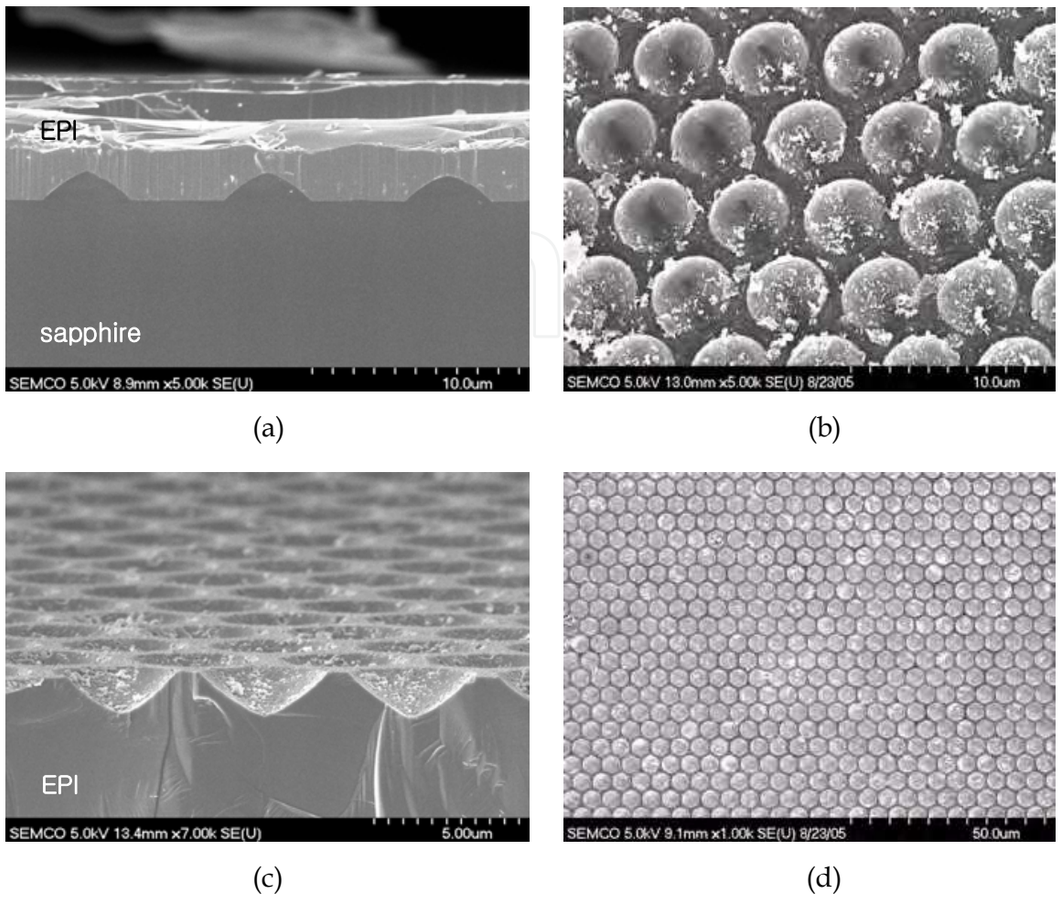


Fig. 10. SEM photographs of top surface (a) LED grown on CSPSS, (b) CSPSS top surface after LLO process, (c) removed n-GaN, (d) after the LLO process

3.6 Surface treatment for higher extraction efficiency

Figure 11 (a) shows the SEM image of the top surface of the concavely patterned undoped-GaN layer after LLO process, transferred from the original CSPSS, with a uniform depth and size. The effective surface area of concavely patterned surface of VT-LED increased to about 50 % compared to that of planar surface VT-LED. The number of the based circle was calculated at about 10,000 based on the interval of ~1 μm and diameter of ~4 μm in 230 × 640 μm² device size (the device is covered with concave pattern about 75% in whole area). This concavely patterned structure reduces also the total internal reflection of the generated light in the active region of the LED and effectively scatters the light outward. For an additional efficiency improvement, concavely patterned surface was further roughened to nano-size dot by etching in 2 M KOH electrolyte at 85 ℃ for 7 min and 15 min, as shown in figure 11(b), (c), respectively. Although circular holes were generated from the initial CSPSS, the chemical etch revealed hexagonal-shaped holes. This is a result of the hexagonal crystal structure of wurtzite GaN. Especially, the concave region shows an open hexagonal inverted pyramid form which is defined by the six {10-1-1} planes.

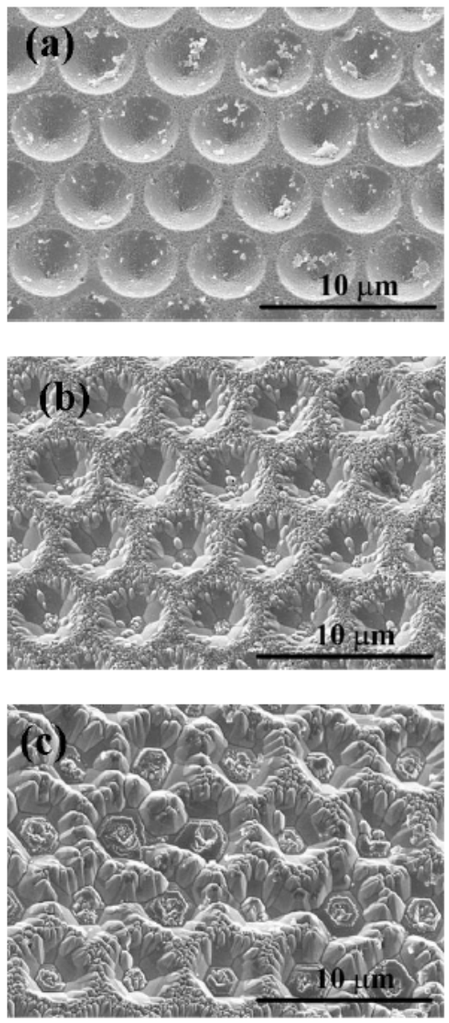


Fig. 11. SEM images of the top surface morphology removed GaN before(a) and after an etching time of 7 min(b) and 15 min(c) in 2M KOH at 85℃, respectively.

3.7 Chip separation using femtosecond laser scribing

Figure 12 shows schematics of a typical heat distribution in the substrate when the substrate is exposed to a focused long pulse and ultra fast short pulse laser beam. As the long pulse laser hits the substrate, the heat generated by the laser power greatly increases the temperature in the vicinity of the focused laser beam spot, locally melting the substrate, and further diffuses away into the material during the pulse duration, because the duration of laser pulse is longer than the heat diffusion time [Liu, et al. 1997; Lee, et al. 2010]. Therefore, the scribing speed is slower and fairly large amount of material droplet remains. However, when an ultrafast laser beam is used for the scribing, which is quite different from those of the long pulse laser beam. As the pulse widths decrease, the laser power intensity easily reaches hundreds of terawatts per square centimeter at the focused beam spot. The heat-affected volume is much smaller because the duration of the laser pulse is shorter than the heat diffusion time. Therefore, the scribing speed is faster and there is no damage.

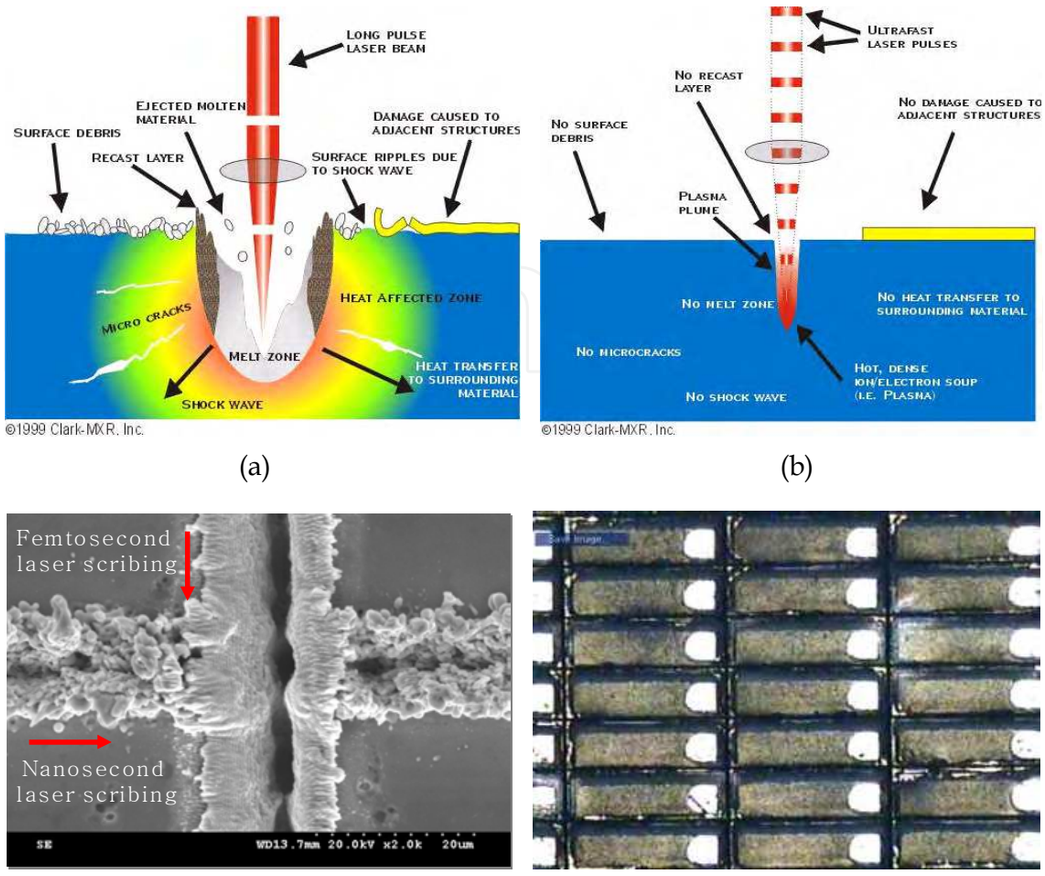


Fig. 12. Schematics of a typical heat distribution in the substrate when the substrate is exposed to a focused long pulse (a) and ultra fast short pulse (b) laser beam. (c) SEM images of the surface of Ni plating substrate after scribing with both nanosecond and femtosecond laser scribing in the same scribing time. (d) Chip separation by using femtosceond laser scribing process.

Figure 12 (c) shows SEM images of the surface of Ni plating substrate after scribing with both nanosecond and femtosecond laser scribing in the same scribing time. The scribing depth of femtosecond laser scribing showed a nearly sevenfold increase compared to that of nanosecond laser scribing. The fabricated VT-LEDs with 230 × 640 μm² size were separated by backside femtosceond laser scribing process as shown in Fig. 12 (d)

3.8 Characteristic of fabricated V-T LED

Figure 13 shows the current-voltage (I-V) characteristics of the fabricated VT-LED with the concavely patterned shape surface. Relatively low forward voltage (Vf =3.2 V) was observed at 20 mA operating current, with a very low reverse leakage current of -4 nA at -5 V. The insert of Fig. 13 shows the fabricated VT-LED with concave-patterned surface and the top view emission image under a driving current of 20 mA. Although it has a long length and the very small n-contact area for application of sideview LED in cellular phone, the current spreading reveals uniform over the total area. Due to a high electron mobility and conductivity

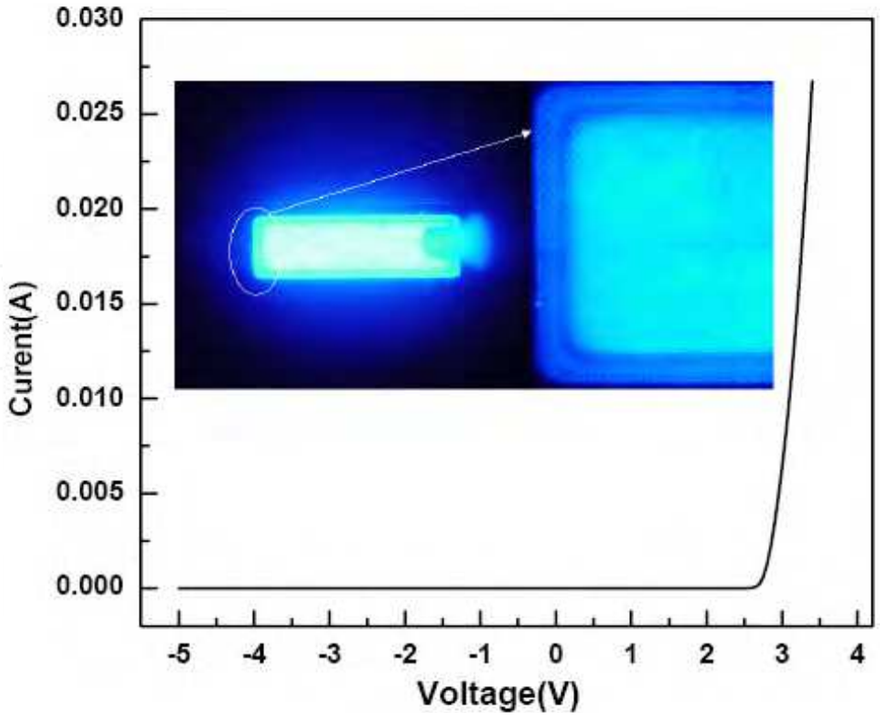


Fig. 13. I-V characteristics of the typical VT-LED. The top view emission images under a driving current of 20 mA in the inset.

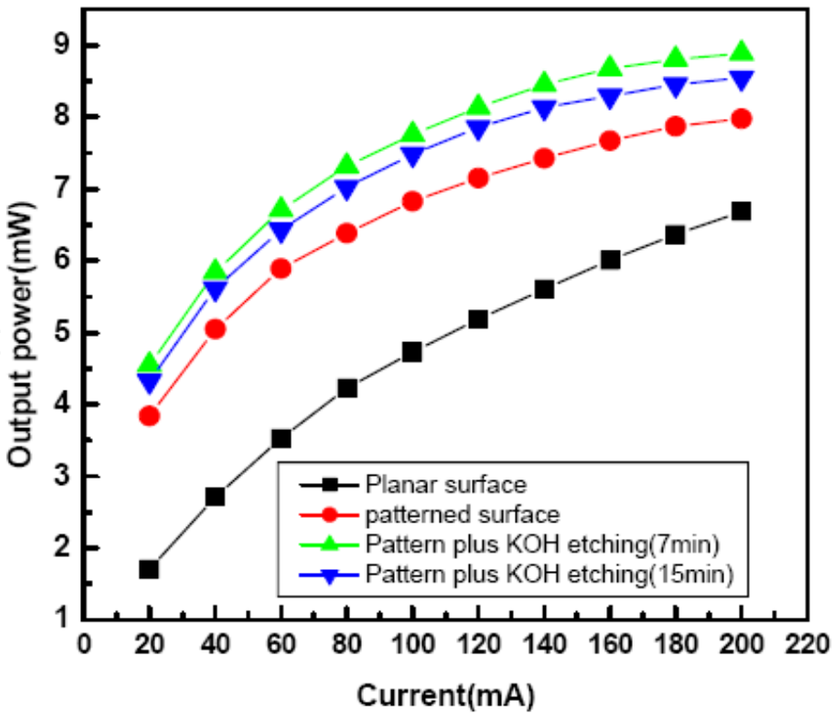


Fig. 14. Light output power of planar surface VT-LEDs and concavely patterned surface VT-LED before and after additional chemical etching in KOH, respectively.

of the n-GaN, the injected electron spreads well in the n-GaN layer without a semitransparent contact layer. Figure 14 shows the light output power as a function of injection current for these four VT-LEDs. The total output power of the devices were measured by using sideview PKG without phosphor to collect the light emitted in all directions from the LEDs. All luminous intensity (L-I) curves showed the slow-saturated characteristics up to 200 mA in relatively small chip size. Because of the higher thermal conductivity of nickel compared to sapphire, these devices are advantageous for high power operation. It should be noted that the output power at 20 mA was estimated to be 1.7, 3.8, 4.5, and 4.3 mW for a planar surface VT-LEDs, concavely patterned surface VT-LED before and after additional chemical etching in KOH, respectively. As compared with the output power for a planar surface VT-LED, the concavely patterned surface VT-LED using HPS plus KOH etching (7 min) resulted in an increase of output power by a factor of 2.7. This significant enhancement in output power could be attributed to the increase of the extraction efficiency, resulted from the increase in photon escaping probability due to enhanced light scattering at the concavely patterned and roughened surface with random nano-size dot.

4. Conclusion

In conclusion, The ELOG–like growth mode on the CSPSS effectively suppresses the probability of dislocation propagation into the cone region and hence greatly improves the crystal quality of the GaN films. The FWHM measured with asymmetric (102) rocking curves decreased from 338 arcsec for InGaN/GaN sample grown on CSS to 225 arcsec in the InGaN/GaN sample grown on CSPSS. To enhance light extraction efficiency, the use of a CSPSS is promising for the cost-effective production of better performing VT-LEDs. The output power of VT-LEDs with a concavely patterned surface is about 3.8 mW at a forward current of 20 mA, which is about 2.2 times higher than the devices with a flat surface. This improvement in the performance of VT-LEDs is attributed to the increase in the escaping probability of photons from the corrugated LED surface as well as the use of metal substrate.

5. Acknowledgment

The author thanks Dr. Jeong-Wook Lee and Mr. In-Suck Choi, Samsung LED Co., LTD., for their useful discussions.

6. References

Amano, H; Sawaki, N.; Akasaki, I. & Toyoda, Y. (1986). Metalorganic vapor phase epitaxial growth of a high quality GaN film using an AlN buffer layer, Appl. Phys. Lett., vol. 48, pp. 353.

Fujii, T.; Gao, Y.; Sharma, R.; Hu, E.L.; DenBaars, S. P. & Nakamura, S. (2004). Increase in the extraction efficiency of GaN-based light-emitting diodes via surface roughening, Appl. Phys. Lett., vol. 84, pp. 855–857.

Gil, B.(1998). Group III Nitride semiconductor Compounds," Clarendon, Oxford.

Grimmeiss, H & Koelmans, Z. H. (1959). Nature, vol. 14, pp. 264.

Huh, C.; Lee, K.S.; Kang E. J. & Park, S.J.(2003). Improved lightoutput and electrical performance of InGaN-based light-emitting diode by microroughening of the p-GaN surface, J. Appl. Phys., vol. 93, no. 11, pp. 9383–9385.

Johnson, W.C; Rasons, J. B & M. C. Crew, (1932). J. Phys. Chem., vol. 234, pp. 2651.

Juza, R; Hahn, H & Allg, Z. A. (1938). Metallic amides and metallic nitrides. V. Crystal structures of Cu3N, GaN and InN, Chem, vol. 234, pp. 282.

Khan, M. A.; Kuania, J. N.; Bhattarai, A.R. & Olsen, D.T. (1993). Metal semiconductor field effect transistor based on single crystal GaN, Appl. Phys. Lett., vol. 62, pp. 1786.

Kittel, C. (1995). Introduction to Solid state physics, 7th Edition, Wiley.

Lee, J. H.; Oh, J.T.; Choi,S.B.;Kim, Y.C.; Cho, H.I. & Lee, J.H.(2008). Enhancement of InGaN-based vertical LED with concavely patterned surface using patterned sapphire substrate," IEEE Photon. Technol. Lett., vol. 20, no. 5, pp. 345–347.

Lee, J. H.; Oh, J.T.; Kim, Y.C & Lee, J.H.(2008). Stress reduction and enhanced extraction efficiency of GaN-based LED grown on cone shape-patterned sapphire, IEEE Photon. Technol. Lett., vol. 20, no. 18, pp. 1563–1565.

Lee, J.H.; Kim, N.S.; Hong, S.S.& Lee, J.H. (2010).Enhanced extraction efficiency of InGaN-based light-emitting diodes using 100 kHz femtosecond-laser-scribing technology, IEEE Electron Device Lett., vol. 31, pp. 213-215.

Lee, J.H.; Lee, D.Y.; Oh, B.W. & Lee, J.H.(2010). Comparison of InGaN-based LEDs grown on conventional sapphire and cone-shapepatterned sapphire substrate, IEEE Trans. Electron Devices, vol. 57, no. 1, pp. 157–163.

Lee, J.H.; Oh, J.T.; Park, J.S.; Kim,J. W.; Kim, Y.C.; Lee, J.W. & Cho, H.K.(2006). Improvement of luminous intensity of InGaN light emitting diodes grown on hemispherical patterned sapphire, Phys. Stat. Sol. (c), vol. 3, pp. 2169–2173.

Levinshtein, M; Rumyantsev, S. & M. Shur, M. (2001). Properties of Advanced Semiconductor Materials, Wiley, New York.

Liu, X.; Du, D. & Mourou, G.(1997). Laser ablation and micromachining with ultrashort laser pulses, IEEE J. Quantum Electron, vol. 33, pp. 1706-1716.; Http://www.cmxr.com.

Look, D.C. & Sizelove, J.R.(2001). Predicted maximum mobility in bulk GaN, Appl. Phys. Lett., vol. 79, pp. 1133.

Maruskam, H. P. & Tietjen, J. J. (1969). The preparation and properties of vapor deposited single crystal line GaN, Appl. Phys. Lett., vol. 15, pp. 327.

Nakamura, S. & G. Fason, G.(1997). The Blue Laser Diode, Sringer, Berlin.

Nakamura, S.(1991). GaN Growth Using GaN Buffer Layer, Jpn. J. Appl. Phys., vol. 30, pp. L1705, 1991.

Nakamura, S.; Senoh, M.; Iwasa, N. & Nagahama, S. (1995). High brightness InGaN blue, green and yellow light-emitting-diodes with quantum well structure, Jpn. J. Appl. Phys., vol. 34, no. 7A, pp. L797–L799.

Nakamura, S.; Senoh, M.; Nagahama, S.; Iwasa, N.; Yamada, T.; Mat-sushita, T.; Sugimoto, Y. & Kiyoku, H. (1997). High-power, long-lifetime InGaN multi-quantum-well-structure laser diodes, Jpn. J. Appl. Phys., vol. 36, no. 8B, pp. L1059–L1061.

Nakamura, S.; Senoh, M.; Nagahoma, S.; Iwasa, N.; Yamada, T.; Matsushita, T.; Kiyoku, H. & Sugimoto, S. (1996). InGaN multi-quantum-well structure laser diodes grown on $MgAl_2O_4$ substrates, Appl. Phys. Lett., vol. 68, pp. 2105.

Ng, H.M.; Doppalapudi, D.; Moustakas, T.D.; Weimann, N.G. & Eastman, L.F.(1998). The role of dislocation scattering in n-type GaN films, Appl. Phys. Lett., vol. 73, pp. 821.

Pankove, J. I. (1997). GaN and Related Materials, Gordon and Breach, New York.

Pankove, J. I.; Chang, S. S.; Lee, H.C.; Molanar, R.; Moustakas, T.D. & Zeghbroeck, B., (1994). High-temperature GaN/SiC heterojunction bipolar transistorwith high gain , Tech. Dig. Int. Electron Devices Meet., vol. 94, pp.389.

Pankove, J. I; Miller, E. A. & Berkeyheiser, J. E. (1972). GaN blue light-emitting diodes, J. Limin. vol. 5, pp. 84.

Ridley, B.K.; Schaff, W.J. & Eastman, L.F. (2004). Hot-phonon-induced velocity saturation in GaN, Appl. Phys. Lett., vol. 96, pp. 1499.

Sakai, A.; Sunakawa, H. & Usui, A. (1997). Defect structure in selectively grown GaN films with low threading dislocation density, Appl. Phys.Lett., vol. 71, no. 16, pp. 2259–2261.

Simeonov, D; Fetin, E; Carlin, J.F.; Ilegems, M. And N. Grandjean, N.(2006). Stranski–Krastanov GaN/AlN quantum dots grown by metal organic vapor phase epitaxy, J. Appl. Phys., vol. 99, pp. 083509.

Smorchkova, I.P.; Keller, S.; Heikman, S.; Elsass, C.R.;Heying, B.; Fini, P.; Speck, J.S. & Mishra, U.K.(2000).Two-dimensional electron-gas AlN/GaN heterostructures with extremely thin AlN barriers, Appl. Phys. Lett., vol. 77, no. 24, pp. 3998–4000.

Sugiura, L.; Itaya, K.; Nishio, J.; Fujimoto, H. & Kokubun, Y.(1997). Effects of thermal treatment of low-temperature GaN buffer layers on the quality of subsequent GaN layers, J. Appl. Phys., vol. 82, pp. 4877–4882.

Sumiya, M,; Ogusu, N.; Yotsuda, Y.; Itoh, M.; Fuke, S.; Nakamura,T.; Mochizuki, S.; Sano, T.; Kamiyama, S.; Amano, H. & Akasaki, I.(2003). Systematic analysis and control of low-temperature GaN buffer layers on sapphire substrates, J. Appl. Phys., vol. 93, pp. 1311–1319.

Tadatomo, K.; Okagawa, H.; Ohuchi, Y.; Tsunekawa, T.; Imada, Y.; Kato, M.& Taguchi, T. (2001). High output power InGaN ultraviolet lightemitting diodes fabricated on patterned substrates using metalorganic vapor phase epitaxy, Jpn. J. Appl. Phys., vol. 40, pp. L583–L585.

Wang, S.J.; Uang, K. M.; Chen, S.L.; Yang, Y. C; Chang, S. C.; Chen, T. M. & Chen, C.H. (2005). Use of patterned laser liftoff process and electroplating nickel layer for the fabrication of vertical-structured GaN-based light-emitting diodes," Appl. Phys. Lett., vol. 87, pp. 011111–011113, 2005.

Wang, W. K.; Huang, S. Y.; Huang, S.H.; Wen, K.S.; Wuu, D.S. & Horng, R.H. (2006).Fabrication and efficiency improvement of micropillar InGaN/Cu light-emitting diodes with vertical electrodes," Appl. Phys. Lett., vol. 88, pp. 181113–181115.

Wraback, M.; Shen, H.; Carrano, J.C.; Li, T.; Campbell, J.C.; Schurman, M.J. & Ferguson, I.T.(2000). Time-resolved electroabsorption measurement of the electron velocity-field characteristic in GaN, Appl. Phys. Lett., vol. 79, pp. 1155.

Wuu, D.S.; Wang, W.K.; Wen, K.S.;Huang, S.C.; Lin, S. H.;Horng, R.H.;Yu,Y.S. & Pan, M.H. (2006). Fabrication of pyramidal patterned sapphire substrates for high-efficiency InGaN-based light emitting diodes, J. Electrochem. Soc., vol. 153, pp. G765–G770.

Yamada, M.; Mitani, T.; Narukawa, Y.; Shioji,S.; Niki, I.; Sonobe, S.; Deguchi, K.; Sano, M. & Mukai, T.(2002). nGaN-based near-ultraviolet and blue-light-emitting diodes with high external quantum efficiency using a patterned sapphire substrate and a mesh electrode, Jpn. J. Appl. Phys., vol. 41, pp. L1431–1433.

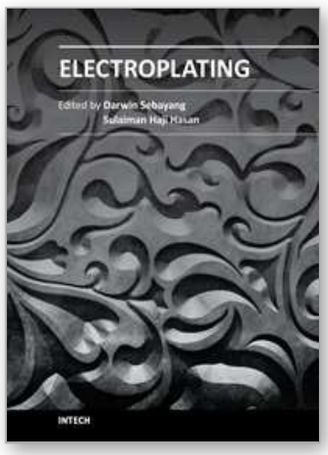
Yoshida, S; Misawa, S. & Gonda, S. (1983). Improvements on the electrical and luminescent properties of reactive molecular beam epitaxially grown GaN films by using AlN coated sapphire substrates, Appl. Phys. Lett., vol. 42, pp. 427.

Youn, D.H.; Lee, J.H.; Kumar, V.; Lee, K.S.; Lee, J.H. & Adesida, I.(2004) The effects of isoelectronic Al doping and process optimization for the fabrication of high-power AlGaN-GaN HEMTs, IEEE Trans. Electron Devices, vol. 51, no. 5, pp. 785–789.

Zheleva,T.S.; Nam, O.H.; Bremser, M.D. and R. F. Davis, R. F.(1997). Dislocation density reduction via lateral epitaxy in selectively grown GaN structures, Appl. Phys. Lett., vol. 71, no. 17, pp. 2472–2474.

IntechOpen

IntechOpen



Electroplating

Edited by Prof. Darwin Sebayang

ISBN 978-953-51-0471-1
Hard cover, 166 pages
Publisher InTech
Published online 11, April, 2012
Published in print edition April, 2012

This book emphasizes on new applications of electroplating with consideration for environmental aspect and experimental design. Written by experienced expert from various countries, the authors come from academia and electroplating industrial players. Here, a very detailed explanation to the new application of the electroplating is followed by a solution of the environmental issue caused by the electroplating process and concluded by experimental design for optimization of electro deposition processes.

Coverage included:
- Preparation NiO catalyst on FeCrAl Subtrate Using Various Technique at Higher Oxidation Process
- Electrochemical properties of carbon- supported metal nanoparticle prepared by electroplating methods
- Fabrication of InGaN-Based Vertical Light Emitting Diodes Using Electroplating
- Integration Of Electrografted Layers for the Metallization of Deep Through Silicon Vias
- Biomass adsorbent for removal of toxic metal ions from electroplating industry wastewater
- Resistant fungal biodiversity of electroplating effluent and their metal tolerance index
- Experimental design and response surface analysis as available tools for statistical modeling and optimization of electrodeposition processes

How to reference

In order to correctly reference this scholarly work, feel free to copy and paste the following:

Jae-Hoon Lee and Jung-Hee Lee (2012). Fabrication of InGaN-Based Vertical Light Emitting Diodes Using Electroplating, Electroplating, Prof. Darwin Sebayang (Ed.), ISBN: 978-953-51-0471-1, InTech, Available from: http://www.intechopen.com/books/electroplating/fabrication-of-ingan-based-vertical-light-emitting-diodes-using-electroplating

INTECH
open science | open minds

InTech Europe
University Campus STeP Ri
Slavka Krautzeka 83/A
51000 Rijeka, Croatia
Phone: +385 (51) 770 447
Fax: +385 (51) 686 166

InTech China
Unit 405, Office Block, Hotel Equatorial Shanghai
No.65, Yan An Road (West), Shanghai, 200040, China
中国上海市延安西路65号上海国际贵都大饭店办公楼405单元
Phone: +86-21-62489820
Fax: +86-21-62489821

www.intechopen.com

IntechOpen

IntechOpen

© 2012 The Author(s). Licensee IntechOpen. This is an open access article distributed under the terms of the Creative Commons Attribution 3.0 License, which permits unrestricted use, distribution, and reproduction in any medium, provided the original work is properly cited.

IntechOpen

IntechOpen